A Cocoon of Freshly Accelerated Cosmic Rays Detected by Fermi in the Cygnus Superbubble

M. Ackermann, *et al.*

Science **334**, 1103 (2011);
DOI: 10.1126/science.1210311

no. DE-AC02-06CH11357. GM/CA CAT has been funded in whole or in part with federal funds from NCI (grant Y1-CO-1020) and NIGMS (grant Y1-GM-1104). Coordinates and structure factors for the Fab PGT 128/Man_9, Fab PGT 127/Man_9, and Fab PGT 128/eODmV3 structures have been deposited with the Protein Data Bank under accession codes 3TV3, 3TWC, and 3TYG. The Fab PGT 128/d664G trimer EM reconstruction density has been deposited with the Electron Microscopy Data Bank under accession code EMD-1970. Progenics Pharmaceuticals and the Cornell Research Foundation, on behalf of Cornell University, are the joint owners of U.S. Patent 7,939,083 and have additional patent applications on the stabilized Env trimer used in this manuscript. The IAVI and Theraclone hold U.S. patent 61/515,528 on the PGT antibodies. The Scripps Research Institute and IAVI have applied for a patent relating to the eODmV3 construct. Materials will be made available for noncommercial use under material transfer agreements with Progenics or Cornell (stabilized Env 664G trimer), IAVI (PGT antibodies), and TSRI (eODmV3). This is manuscript 21407-MB from The Scripps Research Institute.

Supporting Online Material

www.sciencemag.org/cgi/content/full/science.1213256/DC1
Materials and Methods
Figs. S1 to S15
Tables S1 to S6
References (*44*–*78*)

29 August 2011; accepted 6 October 2011
Published online 13 October 2011;
10.1126/science.1213256

A Cocoon of Freshly Accelerated Cosmic Rays Detected by Fermi in the Cygnus Superbubble

M. Ackermann,[1] M. Ajello,[1] A. Allafort,[1] L. Baldini,[2] J. Ballet,[3] G. Barbiellini,[4,5] D. Bastieri,[6,7] A. Belfiore,[8] R. Bellazzini,[2] B. Berenji,[1] R. D. Blandford,[1] E. D. Bloom,[1] E. Bonamente,[9,10] A. W. Borgland,[1] E. Bottacini,[1] M. Brigida,[11,12] P. Bruel,[13] R. Buehler,[1] S. Buson,[6,7] G. A. Caliandro,[14] R. A. Cameron,[1] P. A. Caraveo,[8] J. M. Casandjian,[3] C. Cecchi,[9,10] A. Chekhtman,[15]* C. C. Cheung,[16]* J. Chiang,[1] S. Ciprini,[17,10] R. Claus,[1] J. Cohen-Tanugi,[18] A. de Angelis,[19] F. de Palma,[11,12] C. D. Dermer,[20] E. do Couto e Silva,[1] P. S. Drell,[1] D. Dumora,[21] C. Favuzzi,[11,12] S. J. Fegan,[13] W. B. Focke,[1] P. Fortin,[13] Y. Fukazawa,[22] P. Fusco,[11,12] F. Gargano,[12] S. Germani,[9,10] N. Giglietto,[11,12] F. Giordano,[11,12] M. Giroletti,[23] T. Glanzman,[1] G. Godfrey,[1] I. A. Grenier,[3,24]† L. Guillemot,[25] S. Guiriec,[26] D. Hadasch,[14] Y. Hanabata,[22] A. K. Harding,[27] M. Hayashida,[1] K. Hayashi,[22] E. Hays,[27] G. Jóhannesson,[28] A. S. Johnson,[1] T. Kamae,[1] H. Katagiri,[29] J. Kataoka,[30] M. Kerr,[1] J. Knödlseder,[31,32] M. Kuss,[2] J. Lande,[1] L. Latronico,[2] S.-H. Lee,[33] F. Longo,[4,5] F. Loparco,[11,12] B. Lott,[21] M. N. Lovellette,[20] P. Lubrano,[9,10] P. Martin,[34] M. N. Mazziotta,[12] J. E. McEnery,[27,35] J. Mehault,[18] P. F. Michelson,[1] W. Mitthumsiri,[1] T. Mizuno,[22] C. Monte,[11,12] M. E. Monzani,[1] A. Morselli,[36] I. V. Moskalenko,[1] S. Murgia,[1] M. Naumann-Godo,[3] P. L. Nolan,[1] J. P. Norris,[37] E. Nuss,[18] T. Ohsugi,[38] A. Okumura,[1,39] E. Orlando,[1,34] J. F. Ormes,[40] M. Ozaki,[39] D. Paneque,[41,1] D. Parent,[42]* M. Pesce-Rollins,[2] M. Pierbattista,[3] F. Piron,[18] M. Pohl,[43,44] D. Prokhorov,[1] S. Rainò,[11,12] R. Rando,[6,7] M. Razzano,[2] T. Reposeur,[21] S. Ritz,[45] P. M. Saz Parkinson,[45] C. Sgrò,[2] E. J. Siskind,[46] P. D. Smith,[47] P. Spinelli,[11,12] A. W. Strong,[34] H. Takahashi,[38] T. Tanaka,[1] J. G. Thayer,[1] J. B. Thayer,[1] D. J. Thompson,[27] L. Tibaldo,[6,7,3]† D. F. Torres,[14,48] G. Tosti,[9,10] A. Tramacere,[1,49,50] E. Troja,[28] Y. Uchiyama,[1] J. Vandenbroucke,[1] V. Vasileiou,[18] G. Vianello,[1,49] V. Vitale,[37,51] A. P. Waite,[1] P. Wang,[1] B. L. Winer,[47] K. S. Wood,[20] Z. Yang,[52,53] S. Zimmer,[52,53] S. Bontemps[54]

The origin of Galactic cosmic rays is a century-long puzzle. Indirect evidence points to their acceleration by supernova shockwaves, but we know little of their escape from the shock and their evolution through the turbulent medium surrounding massive stars. Gamma rays can probe their spreading through the ambient gas and radiation fields. The Fermi Large Area Telescope (LAT) has observed the star-forming region of Cygnus X. The 1- to 100-gigaelectronvolt images reveal a 50-parsec-wide cocoon of freshly accelerated cosmic rays that flood the cavities carved by the stellar winds and ionization fronts from young stellar clusters. It provides an example to study the youth of cosmic rays in a superbubble environment before they merge into the older Galactic population.

Isotopic and elemental abundances indicate that ~20% of the cosmic-ray (CR) nuclei are synthesized by massive Wolf-Rayet stars at least 10^5 years before their acceleration, presumably by a supernova shockwave (*1*–*3*). Massive stars cluster in space and time (*4*). Their supersonic winds and explosions power fast shockwaves and supersonic turbulence in the surrounding medium; thus, particle confinement and reacceleration by repeated shocks can substantially modify the CR properties before they diffuse at large in the Galaxy (*5*, *6*). This early diffusion can be followed in γ rays as the young CRs interact with the gas and radiation surrounding stellar clusters.

The Cygnus X region boasts an abundance of massive stars born in the past few million years in numerous associations (*7*), notably in the massive Cyg OB2 cluster at a distance of 1.4 kpc (*8*, *9*). The bright clusters have sculpted their parent molecular clouds over tens of parsecs (*10*, *11*) through ionization, radiation pressure, and expansion of the coalescing stellar winds, creating lower-density cavities filled with neutral and ionized hydrogen from photodissociated H_2. The compressed edges along the ionization fronts shine brightly in midinfrared as photon-dominated regions (PDRs) (Fig. 1). The presence of the γ Cygni supernova remnant in the region (*12*) and the detection of diffuse TeV emission by Milagro (*13*, *14*) suggest the potential presence of young CRs. We probed their properties with Fermi Large Area Telescope (LAT) observations in the 0.1- to 100-GeV energy band at Galactic longitudes $72° \leq l \leq 88°$ and latitudes $|b| \leq 15°$.

We modeled the spatial and spectral distributions of the interstellar radiation (*15*, *16*) as a linear combination of gas contributions from different clouds seen along the lines of sight in the atomic, molecular, and dark neutral gas phases (fig. S1). We added a contribution from the large-scale Galactic inverse Compton (IC) emission, an isotropic intensity for the instrumental and extragalactic backgrounds, and several noninterstellar sources such as pulsars and supernova remnants. In particular, we detected hard emission above 3 GeV from γ Cygni (figs. S2 and S3), and the extended source was added to the background model (Fig. 2).

The 0.1- to 100-GeV data indicate that the 8 million solar masses of gas of the whole Cygnus complex are, on average, pervaded by the same CR flux and spectrum as near the Sun (*15*), to within 20%. In the central regions, toward Cygnus X, the molecular clouds may exhibit a slightly harder spectrum above 10 GeV than the surrounding atomic clouds, but the deviation significance is $<3\sigma$ (*15*), so our background model assumes the same spectrum in all gas phases unless otherwise mentioned.

We find an extended excess of hard emission above the modeled background (Fig. 2C). The excess fades out below 1 GeV because of the steep rise of the softer gas components (*15*). To measure the significance and spectrum of the excess, we fitted a Gaussian source with free location and width. The best fit ($l = 79.6° \pm 0.3°$, $b = 1.4° \pm 0.4°$, $\sigma = 2.0° \pm 0.2°$) (fig. S4) yields a 10.1 σ detection above 1 GeV. We get a comparable significance and consistent morphology

when allowing the spectrum of the central molecular clouds to harden above 10 GeV or when changing the HI spin temperature in the background model (*16*).

The zoom in Fig. 3A shows how the excess emission relates to the interstellar structures in Cygnus X. It stretches over ~50 pc between Cyg OB2 and γ Cygni, in the cavity fringed by PDRs.

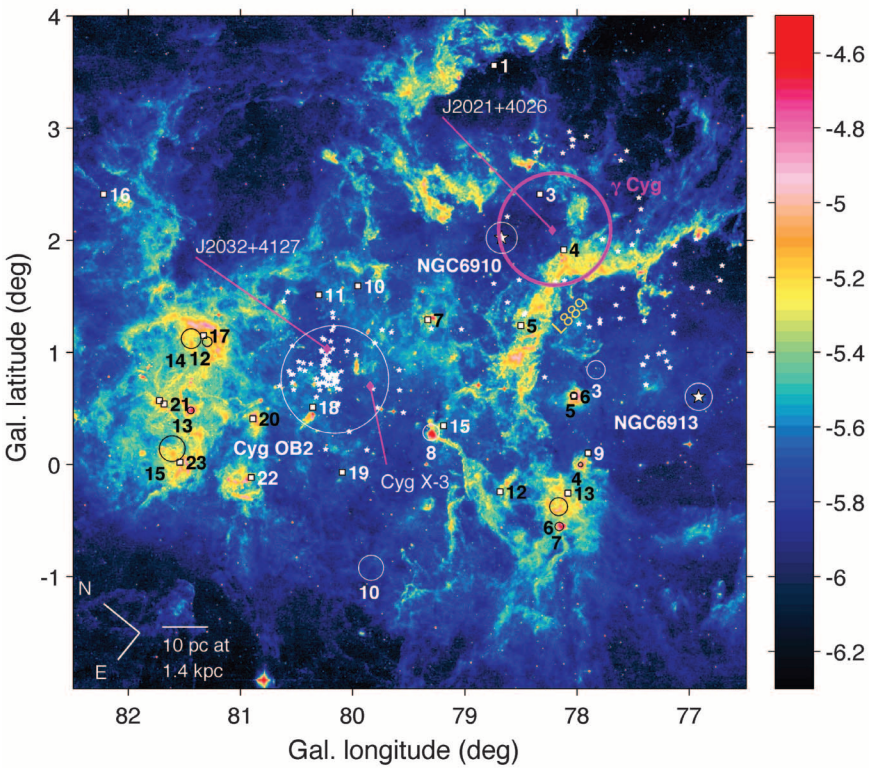

Fig. 1. An 8-μm intensity map of the Cygnus X region from MSX (W m^{-2} sr^{-1}, in log scale), outlining the PDRs. Objects are noted with their names or numbers: Cyg X-3 and pulsars J2021+4026 and J2032+4127 (magenta diamonds); the γ Cygni supernova remnant (magenta circle); OB associations [white or black circles (*7*)]; HII regions [white squares (*10*)]; and OB stars from Cyg OB2 and Cyg OB9 [white stars (*8*, *29*)].

The well-resolved morphology extends far beyond the sizes of Cyg OB2 and γ Cygni, and it differs from the spatial distributions of the various gas phases (fig. S1). It distinctly follows the regions bounded by PDRs, as in a cocoon. The emission peaks toward massive-star clusters (NGC6910, the western part of Cyg OB2, and associations circled in Fig. 1) and toward the southernmost molecular cloud. Stellar clusters can host γ-ray point sources, but the smooth radial profile of the excess (fig. S5), the comparable spectra obtained in different parts (fig. S6), the poorer fit obtained with an ensemble of discrete point sources (*16*) (fig. S4), and the spatial relation with PDRs, all point to the diffuse, interstellar origin of the excess emission.

Pulsar wind nebulae power extended γ-ray sources, but the young pulsars J2021+4026 in γ Cygni and J2032+4127 are unlikely to explain the cocoon emission (*16*). We cannot rule out a yet-undiscovered nebula, but the close relation between the emission morphology and the interstellar structure in Cygnus X favors a CR origin.

The hard cocoon emission extends to 100 GeV (Fig. 4). The flux of $(5.8 \pm 0.9) \times 10^{-8}$ cm^{-2} s^{-1} in the 1- to 100-GeV band gives a luminosity of $(9 \pm 2) \times 10^{27}$ W at 1.4 kpc, which represents only ~0.03% and ~7% of the stellar wind power in Cyg OB2 and NGC 6910, respectively (*16*). The cocoon overlaps the source MGRO J2031+41 (*14*), and the flux above 10 TeV appears consistent with the extrapolation of the LAT data (Fig. 4) (*13*).

Ionized gas was not part of the background model and can be traced by free-free emission at 40 GHz (*16*). We derived N(HII) column densities for a temperature of 10^4 K and different electron effective densities n_{eff} (*17*). The cocoon

[1]W. W. Hansen Experimental Physics Laboratory, Kavli Institute for Particle Astrophysics and Cosmology, Department of Physics and SLAC National Accelerator Laboratory, Stanford University, Stanford, CA 94305, USA. [2]Istituto Nazionale di Fisica Nucleare, Sezione di Pisa, I-56127 Pisa, Italy. [3]Laboratoire AIM, CEA-IRFU/CNRS/Université Paris Diderot, Service d'Astrophysique, CEA Saclay, 91191 Gif sur Yvette, France. [4]Istituto Nazionale di Fisica Nucleare, Sezione di Trieste, I-34127 Trieste, Italy. [5]Dipartimento di Fisica, Università di Trieste, I-34127 Trieste, Italy. [6]Istituto Nazionale di Fisica Nucleare, Sezione di Padova, I-35131 Padova, Italy. [7]Dipartimento di Fisica "G. Galilei," Università di Padova, I-35131 Padova, Italy. [8]INAF-Istituto di Astrofisica Spaziale e Fisica Cosmica, I-20133 Milano, Italy. [9]Istituto Nazionale di Fisica Nucleare, Sezione di Perugia, I-06123 Perugia, Italy. [10]Dipartimento di Fisica, Università degli Studi di Perugia, I-06123 Perugia, Italy. [11]Dipartimento di Fisica "M. Merlin" dell'Università e del Politecnico di Bari, I-70126 Bari, Italy. [12]Istituto Nazionale di Fisica Nucleare, Sezione di Bari, 70126 Bari, Italy. [13]Laboratoire Leprince-Ringuet, École Polytechnique, CNRS/IN2P3, Palaiseau, France. [14]Institut de Ciències de l'Espai (IEEE-CSIC), Campus UAB, 08193 Barcelona, Spain. [15]Artep Inc., 2922 Excelsior Springs Court, Ellicott City, MD 21042, USA [16]National Research Council Research Associate, National Academy of Sciences, Washington, DC 20001, USA. [17]Agenzia Spaziale Italiana (ASI) Science Data Center, I-00044 Frascati (Roma), Italy. [18]Laboratoire Univers et Particules de Montpellier, Université Montpellier 2, CNRS/IN2P3, Montpellier, France. [19]Dipartimento di Fisica, Università di Udine and Istituto Nazionale di Fisica Nucleare, Sezione di Trieste, Gruppo Collegato di Udine, I-33100 Udine, Italy. [20]Space Science Division, Naval Research Laboratory, Washington, DC 20375–5352, USA. [21]Université Bordeaux 1, CNRS/IN2p3, Centre d'É tudes Nucléaires de Bordeaux Gradignan, 33175 Gradignan, France. [22]Department of Physical Sciences, Hiroshima University, Higashi-Hiroshima, Hiroshima 739-8526, Japan. [23]INAF Istituto di Radioastronomia, 40129 Bologna, Italy. [24]Institut Universitaire de France, France. [25]Max-Planck-Institut für Radioastronomie, Auf dem Hügel 69, 53121 Bonn, Germany. [26]Center for Space Plasma and Aeronomic Research (CSPAR), University of Alabama in Huntsville, Huntsville, AL 35899, USA. [27]NASA Goddard Space Flight Center, Greenbelt, MD 20771, USA. [28]Science Institute, University of Iceland, IS-107 Reykjavik, Iceland. [29]College of Science, Ibaraki University, 2-1-1, Bunkyo, Mito 310-8512, Japan. [30]Research Institute for Science and Engineering, Waseda University, 3-4-1, Okubo, Shinjuku, Tokyo 169-8555, Japan. [31]CNRS, Research Institute in Astrophysics and Planetology (IRAP), F-31028 Toulouse cedex 4, France. [32]Université de Toulouse, UPS-OMP, IRAP, Toulouse, France. [33]Yukawa Institute for Theoretical Physics, Kyoto University, Kitashirakawa Oiwake-cho, Sakyo-ku, Kyoto 606-8502, Japan. [34]Max-Planck Institut für Extraterrestrische Physik, 85748 Garching, Germany. [35]Department of Physics and Department of Astronomy, University of Maryland, College Park, MD 20742, USA. [36]Istituto Nazionale di Fisica Nucleare, Sezione di Roma "Tor Vergata", I-00133 Roma, Italy. [37]Department of Physics, Boise State University, Boise, ID 83725, USA. [38]Hiroshima Astrophysical Science Center, Hiroshima University, Higashi-Hiroshima, Hiroshima 739-8526, Japan. [39]Institute of Space and Astronautical Science, JAXA, 3-1-1 Yoshinodai, Chuo-ku, Sagamihara, Kanagawa 252-5210, Japan. [40]Department of Physics and Astronomy, University of Denver, Denver, CO 80208, USA. [41]Max-Planck-Institut für Physik, D-80805 München, Germany. [42]Center for Earth Observing and Space Research, College of Science, George Mason University, Fairfax, VA 22030, USA. [43]Institut für Physik und Astronomie, Universität Potsdam, 14476 Potsdam, Germany. [44]Deutsches Elektronen Synchrotron DESY, D-15738 Zeuthen, Germany. [45]Santa Cruz Institute for Particle Physics, Department of Physics and Department of Astronomy and Astrophysics, University of California at Santa Cruz, Santa Cruz, CA 95064, USA. [46]NYCB Real-Time Computing Inc., Lattingtown, NY 11560–1025, USA. [47]Department of Physics, Center for Cosmology and Astro-Particle Physics, The Ohio State University, Columbus, OH 43210, USA. [48]Institució Catalana de Recerca i Estudis Avançats (ICREA), Barcelona, Spain. [49]Consorzio Interuniversitario per la Fisica Spaziale (CIFS), I-10133 Torino, Italy. [50]INTEGRAL Science Data Centre, CH-1290 Versoix, Switzerland. [51]Dipartimento di Fisica, Università di Roma "Tor Vergata", I-00133 Roma, Italy. [52]Department of Physics, Stockholm University, AlbaNova, SE-106 91 Stockholm, Sweden. [53]The Oskar Klein Centre for Cosmoparticle Physics, AlbaNova, SE-106 91 Stockholm, Sweden. [54]Laboratoire d'Astrophysique de Bordeaux, Université de Bordeaux, CNRS/INSU, Floirac cedex, France.

*Resident at Naval Research Laboratory, Washington, DC 20375, USA.
†To whom correspondence should be addressed. E-mail: isabelle.grenier@cea.fr (I.A.G.); luigi.tibaldo@pd.infn.it (L.T.)

encloses 3.2×10^4 (n_{eff}/10 cm^{-3})$^{-1}$ solar masses of ionized gas at 1.4 kpc (fig. S1D). However, the mass is an order of magnitude too low and the "Local" CR spectrum (i.e., that near the Sun) is too soft to explain the LAT data (Fig. 4). The cocoon partially overlaps a concentration of ionized gas (fig. S1D). We fitted the N(HII) map to the data in addition to the other interstellar components. The template is significantly detected, but at the expense of an unusually large emissivity, much harder than in the other gas phases (*15*). Its spectrum compares well with that extracted with the 2° Gaussian source (fig. S7). Thus, overlooked gas in any state, illuminated by the same CR spectrum as found in the rest of the region, cannot explain the observed hardness of the cocoon emission. It requires a harder CR spectrum.

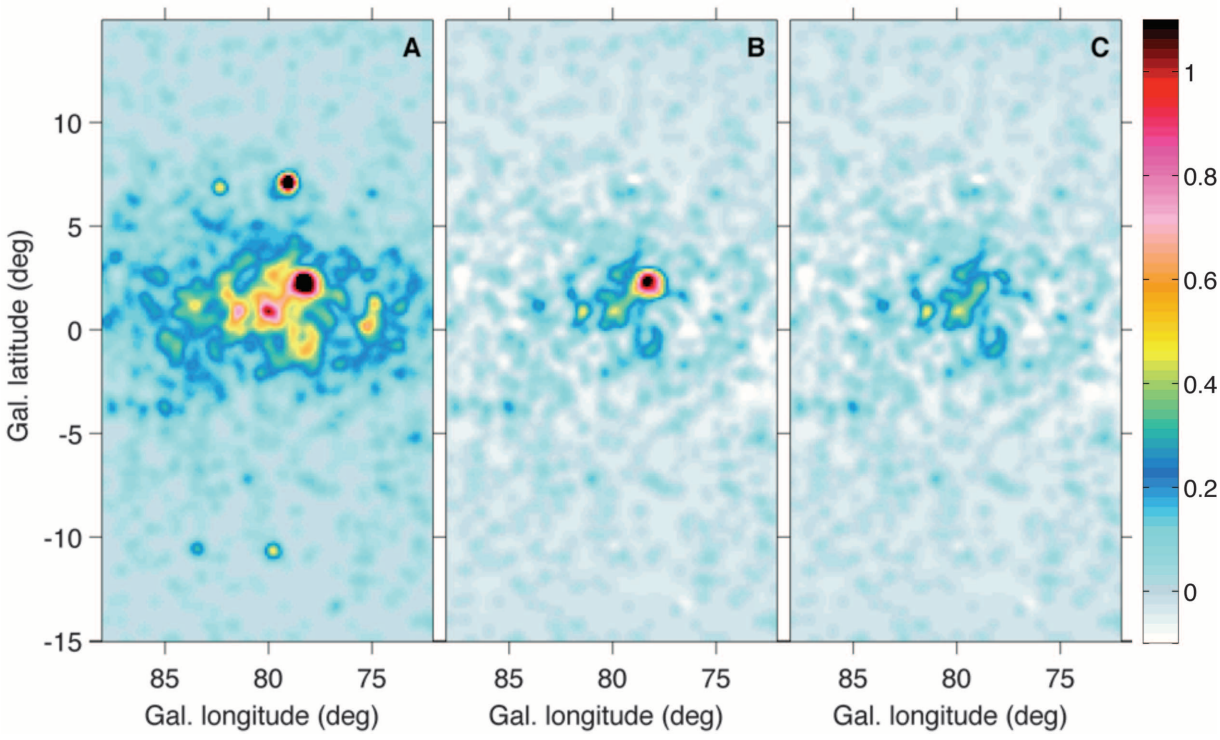

Fig. 2. Photon count maps in the 10- to 100-GeV band (*30*), smoothed with a σ = 0.25° Gaussian kernel, obtained for the total emission (**A**), after subtraction of the interstellar background and all known sources but γ Cygni (**B**), and after further removal of the extended emission from γ Cygni (**C**).

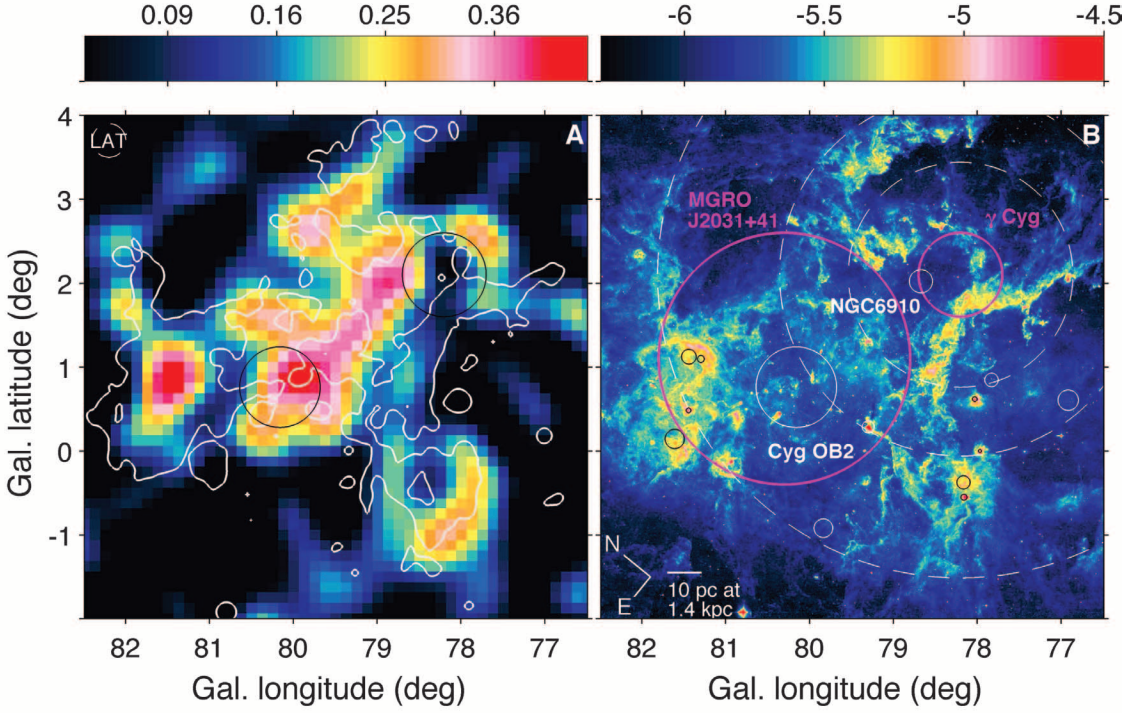

Fig. 3. (**A**) Photon count residual map in the 10- to 100-GeV band (*30*), smoothed with a σ = 0.25° Gaussian kernel, and overlaid with the $10^{-5.6}$ W m^{-2} sr^{-1} white contour of the 8-μm intensity. The typical LAT angular resolution above 10 GeV is indicated. The black circles mark γ Cygni and Cyg OB2. (**B**) An 8-μm map and solid circles for γ Cygni and stellar clusters, as in Fig. 1. The large magenta circle marks the location and extent of the source MGRO J2031+41 (*14*); dashed circles give upper limits to the diffusion lengths of 10, 10^2, and 10^3 GeV particles after 5000 years of travel time using the standard interstellar diffusion coefficient. Their origin from the position of the rim of γ Cygni 5000 years ago is purely illustrative.

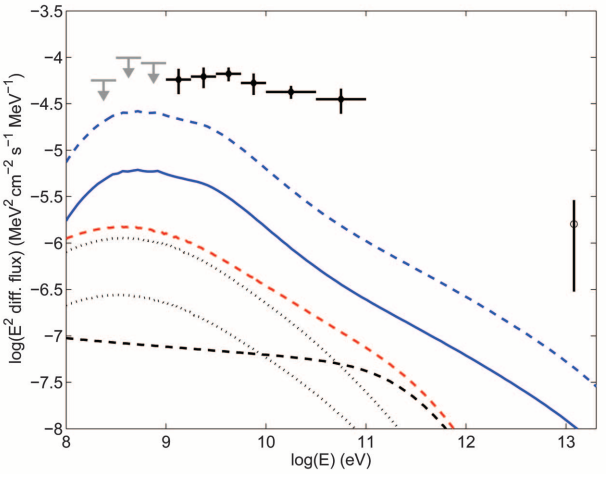

Fig. 4. Energy spectrum of the cocoon emission. The 1σ errors are statistical; 2σ upper limits are given below 1 GeV. The Milagro flux (open circle), integrated over 78.7° < l < 81.7° and −0.4° < *b* <2.6°, is corrected for the extrapolation of the TeV J2032+4130 source at energies >10 TeV. The blue curves show the expectations from the Local CR spectrum pervading the ionized gas for electron densities n_{eff} = 10 cm^{-3} (solid) and 2 cm^{-3} (dashed). The black curves give the expectations from the Local CR electron spectrum upscattering the stellar light from Cyg OB2 (upper dotted curve), NGC 6910 (lower dotted curve), and the interstellar radiation present in the cavity and PDRs (dashed curve). The red curve sums all IC emissions.

To reproduce the LAT data with pure hadronic emission (*16*), we need an amplification factor of (1.6 to 1.8) × (E/10 GeV)$^{0.3}$ of the Local proton and helium spectra in the cocoon. It implies a total CR energy of 1.3 × 10^{42} J above 2 GeV/nucleon and a volume energy density 50% larger than that near the Sun.

We calculated an upper bound to the IC emission expected from CR electrons, with the Local spectrum, upscattering the stellar light from Cyg OB2 and NGC6910 (*16*). The enhanced, infrared-rich, interstellar radiation field (ISRF) in the region (fig. S8) also provides hard IC emission in addition to the cluster contributions and to the Galactic component included in the background model. We used radio to infrared maps, the Local electron spectrum, and a 25-pc (1°) thickness along the lines of sight to estimate the ISRF and IC spectra in each pixel subtended by the cocoon (*16*). We added stellar light fields to account for the average abundance of stars outside Cyg OB2 and NGC6910. The total IC emission, integrated over the cocoon directions, is too faint and too soft to match the data (Fig. 4). An amplification factor of 60 × (E/10 GeV)$^{0.5}$ of the Local electron spectrum can, for instance, account for the LAT data without overpredicting the average synchrotron intensity we measured at 0.408 and 1.42 GHz in the cocoon. The synchrotron calculation used a magnetic field of 2 nT deduced from pressure balance with the gas. The amplified electron spectrum gives a total energy of 4 × 10^{41} J above 1 GeV.

Whether CR electrons or nuclei dominate the cocoon γ radiation, its hardness points to freshly accelerated particles. TeV electrons have a 20,000-year lifetime against synchrotron and IC losses in the cocoon environment (with average magnetic and ISRF energy densities of 9.9 and 6.8 MeV m^{-3}, respectively). A hard pion spectrum indicates nuclei having recently left their accelerator. After a travel time τ, particles diffuse to a characteristic length $L_{2D} = [4\,D(E)\,\tau]^{1/2}$ for an interstellar diffusion coefficient D(E) = 10^{24} (E/10 GeV)$^{1/2}$ m^2/s. They can flood the entire cocoon in a few thousand years from a single accelerator anywhere in Cygnus X, with higher-energy particles reaching farther out (Fig. 3B). The fact that we obtain consistent widths for the Gaussian source in the 1 to 10 and 10 to 100 GeV bands, however, suggests an efficient confinement inside the cocoon.

We conclude that the cavities carved by the young stellar clusters form a cocoon of hard CRs. It provides evidence for the long-advocated hypothesis that OB associations host CR factories.

Where is/are the accelerator(s)? γ Cygni is a potential candidate. Its relation to the Cygnus X cavities is unclear. It expands in low gas densities [0.3 cm^{-3} (*18*)], but a chance alignment in this crowded direction is possible. γ Cygni shelters energetic particles shining in γ rays (figs. S2 and S3). We used the present expansion characteristics of the 7000-year-old shockwave to follow its past evolution and to evaluate the energy the particles could reach by Fermi acceleration at the end of the free expansion phase, 5000 years ago (*16*). With CR pressure feedback on the shock and magnetic amplification by the streaming CRs, we obtain maximum energies of 80 to 300 TeV for protons and 6 to 50 TeV for the radiating electrons (*16*). These values are high enough to explain the LAT emission with nuclei and/or electron emission after a few thousand years of interstellar propagation, but not the Milagro flux with pure IC emission. The anisotropy of the emission around the supernova remnant challenges this scenario. The slightly foreground molecular ridge extending southeast of the remnant (along L889 and HII region 4) may be too far to serve as a target mass (*10*). Another option involves a champagne flow (*19*, *20*) with the shockwave breaking away into a cavity and advecting particles out, independent of their energy, but there is no evidence that the shockwave of γ Cygni rushes out on its eastern rim (*12*). In the absence of advection, the short diffusion lengths expected in the turbulent medium of Cygnus X (see below) may rule out the very young γ Cygni as the unique accelerator in the cocoon.

OB associations are considered as CR accelerators from the collective action of multiple shocks from supernovae and the winds of massive stars [e.g., (*5*, *6*, *21*–*23*)]. The age of Cyg OB2, spreading from $3.5^{+0.75}_{-1.0}$ million years in the core to $5.25^{+1.5}_{-1.0}$ million years in the northwest (*9*), allows the production of very few supernovae, if any. NGC6910 has a comparable age of 6 ± 2 million years (*24*). We applied the superbubble acceleration formalism (*5*) solely to the termination shocks of random winds in the high gas pressure (10^{-12} Pa) of the cocoon (*16*). Their characteristic size and mean separation of ~10 pc is taken as the energy-containing scale of the strong magnetic turbulence (*16*). It leads to diffusion lengths that are shorter by a factor of 100 than in the standard interstellar medium; thus, protons can remain confined over 100,000 years in agreement with the time scale implied by isotopic abundances (*1*, *25*). Their energy distribution peaks at 10 to 100 GeV and extends to 150 TeV, so their γ radiation in the ambient gas can explain the hard cocoon spectrum (*16*). It is therefore possible that the cocoon is an active CR superbubble. It provides a test case to study the impact of wind-powered turbulence on CR diffusion and its potential for acceleration, both for in situ CR production and to energize Galactic CRs passing in the tangled environment of star-forming regions. Small γ-ray spectral variations across the cocoon can point to a single accelerator or to a distributed acceleration within the superbubble.

A dozen outstanding stellar clusters, at least as young and rich as Cyg OB2, are known in the Galaxy [e.g., (*9*)]. The production and confinement of fresh CRs in the Cygnus X cocoon provides an alternative scenario on the origin of the TeV emission seen toward several of these clusters [the Arches, Quintuplet, and Sgr B2 (*26*), Westerlund 2 (*27*), and Westerlund 1 (*28*)].

References and Notes

1. M. E. Wiedenbeck *et al.*, *Astrophys. J.* **523**, L61 (1999).
2. W. R. Binns *et al.*, *Astrophys. J.* **634**, 351 (2005).
3. J. C. Higdon, R. E. Lingenfelter, *Astrophys. J.* **590**, 822 (2003).
4. A. Blaauw, *Annu. Rev. Astron. Astrophys.* **2**, 213 (1964).
5. A. M. Bykov, I. N. Toptygin, *Astron. Lett.* **27**, 625 (2001).
6. E. Parizot, A. Marcowith, E. van der Swaluw, A. M. Bykov, V. Tatischeff, *Astron. Astrophys.* **424**, 747 (2004).
7. J. M. Le Duigou, J. Knödlseder, *Astron. Astrophys.* **392**, 869 (2002).
8. M. M. Hanson, *Astrophys. J.* **597**, 957 (2003).
9. N. J. Wright, J. J. Drake, J. E. Drew, J. S. Vink, *Astrophys. J.* **713**, 871 (2010).
10. N. Schneider *et al.*, *Astron. Astrophys.* **458**, 855 (2006).
11. A. Roy *et al.*, *Astrophys. J.* **727**, 114 (2011).
12. Y. Ladouceur, S. Pineault, *Astron. Astrophys.* **490**, 197 (2008).
13. A. A. Abdo *et al.*, *Astrophys. J.* **658**, L33 (2007).
14. A. A. Abdo *et al.*, *Astrophys. J.* **664**, L91 (2007).
15. Fermi LAT Collaboration, *Astron. Astrophys.*, arXiv:1110.6123 (2011).

16. Materials and methods are available as supporting material on *Science* Online.
17. T. J. Sodroski *et al.*, *Astrophys. J.* **480**, 173 (1997).
18. T. A. Lozinskaya, V. V. Pravdikova, A. V. Finoguenov, *Astron. Lett.* **26**, 77 (2000).
19. H. J. Völk, *Space Sci. Rev.* **36**, 3 (1983).
20. I. A. Grenier, *30th Int. Cosmic Ray Conf.* **6**, 133 (2008)
21. T. Montmerle, *Astrophys. J.* **231**, 95 (1979).
22. C. Cesarsky, T. Montmerle, *Space Sci. Rev.* **36**, 173 (1983).
23. G. Ferrand, A. Marcowith, *Astron. Astrophys.* **510**, A101 (2010).
24. Z. Kołaczkowski *et al.*, *Acta Astronomica* **54**, 33 (2004).
25. W. R. Binns *et al.*, *N. Astron. Rev.* **52**, 427 (2008).
26. F. A. Aharonian *et al.*, *Nature* **439**, 695 (2006).
27. HESS Collaboration *et al.*, *Astron. Astrophys.* **525**, A46 (2011).
28. S. Ohm *et al.*, 25th Texas Symposium on Relativistic Astrophysics (2010); http://pos.sissa.it/cgi-bin/reader/conf.cgi?confid=123
29. SIMBAD Astronomical Database, CDS Strasbourg, http://simbad.u-strasbg.fr/simbad
30. Images are presented above 10 GeV where the imaging performance is highest (*16*).

Acknowledgments: The Fermi LAT Collaboration acknowledges support from a number of agencies and institutes for both development and the operation of the LAT as well as scientific data analysis. These include NASA and the Department of Energy in the United States; Commissariat à l'Energie Atomique et aux Énergies Alternatives, Institut de Recherche sur les Lois Fondamentales de l'Univers (CEA/IRFU) and Institut National de Physique Nucléaire et de Physique des Particules, Centre National de la Recherche Scientifique (IN2P3/CNRS) in France; Agenzia Spaziale Italiana (ASI) and Istituto Nazionale di Fisica Nucleare (INFN) in Italy; Ministry of Education, Culture, Sports, Science, and Technology (MEXT), Energy Accelerator Research Organization (KEK), and Japan Aerospace Exploration Agency (JAXA) in Japan; and the K. A. Wallenberg Foundation, Swedish Research Council, and National Space Board in Sweden. Additional support from Istituto Nazionale di Astrofisica (INAF) in Italy and Centre National d'Etudes Spaciales (CNES) in France for science analysis during the operations phase is also gratefully acknowledged. L.T. is partially supported by the International Doctorate on Astroparticle Physics (IDAPP) program. E.T is a NASA Postdoctoral Program Fellow.

Supporting Online Material

www.sciencemag.org/cgi/content/full/334/6059/1103/DC1
Materials and Methods
Figs. S1 to S8
Tables S1 to S3
References (*31*–*67*)

24 June 2011; accepted 28 October 2011
10.1126/science.1210311

Fermi Detection of a Luminous γ-Ray Pulsar in a Globular Cluster

The Fermi LAT Collaboration*†

We report on the Fermi Large Area Telescope's detection of γ-ray (>100 mega–electron volts) pulsations from pulsar J1823–3021A in the globular cluster NGC 6624 with high significance (~7 σ). Its γ-ray luminosity, $L_\gamma = (8.4 \pm 1.6) \times 10^{34}$ ergs per second, is the highest observed for any millisecond pulsar (MSP) to date, and it accounts for most of the cluster emission. The nondetection of the cluster in the off-pulse phase implies that it contains <32 γ-ray MSPs, not ~100 as previously estimated. The γ-ray luminosity indicates that the unusually large rate of change of its period is caused by its intrinsic spin-down. This implies that J1823–3021A has the largest magnetic field and is the youngest MSP ever detected and that such anomalous objects might be forming at rates comparable to those of the more normal MSPs.

Since its launch in 2008, the Large Area Telescope (LAT) on board the Fermi Gamma-ray Space Telescope (*1*) has detected whole populations of objects previously unseen in the γ-ray band. These include globular clusters (GCs), which are ancient spherical groups of ~10^5 stars held together by their mutual gravity. As a class, their γ-ray spectra show evidence for an exponential cut-off at high energies (*2*, *3*), a characteristic signature of magnetospheric pulsar emission. This is not surprising because radio surveys have shown that GCs contain large numbers of pulsars (*4*), neutron stars that emit radio and in some cases x-ray and γ-ray pulsations.

The first GC detected at γ-ray energies was 47 Tucanae (*5*), soon followed by Terzan 5 (*6*) and nine others (*2*, *3*). Even so, no individual pulsars in these clusters were firmly identified in γ-rays (*7*). GCs are more distant than most γ-ray pulsars observed in the Galactic disk (*8*); thus, most pulsars in them should be too faint to be detected individually. The Fermi LAT lacks the spatial resolution required to resolve the pulsars in GCs, which tend to congregate within the inner arcminute of the cluster. Hence, γ-ray photons emitted by all pulsars in a given GC increase the photon background in the folded γ-ray profiles of each individual pulsar in that cluster.

One of the GCs detected at γ-ray energies is NGC 6624 (*3*), located at a distance $d = 8.4 \pm 0.6$ kpc from Earth (*9*). With a radio flux density at 400 MHz of $S_{400} = 16$ mJy, J1823–3021A is the brightest of the six pulsars known in the cluster. It has been regularly timed with the Jodrell Bank and Parkes radio telescopes since discovery and with the Nançay radio telescope since the launch of the Fermi satellite. The resulting radio ephemeris (table S1) describes the measured pulse times of arrival very well for the whole length of the Fermi mission, the root mean square of the timing residuals being 0.1% of the pulsar rotational period.

Thus, we can confidently use it to assign a pulsar spin phase φ to every γ-ray (>0.1 GeV) photon arriving at the Fermi LAT from the direction (within 0.8°) of the pulsar. We selected photons that occurred between 4 August 2008 and 4 October 2010 that pass the "Pass 6 diffuse" γ-ray selection cuts (*1*). The resulting pulsed γ-ray signal (above 0.1 GeV) (Fig. 1) is very robust, with an H-test value of 64 (*10*), corresponding to 6.8 σ significance. The data are well modeled by a power law with spectral index 1.4 ± 0.3 and an exponential cut-off at an energy of 1.3 ± 0.6 GeV, typical of the values found for other γ-ray pulsars [see supporting online material (SOM)]. The two peaks are aligned, within uncertainties, with the two main radio components at spin phases $\phi_1 = 0.01 \pm 0.01$ and $\phi_2 = 0.64 \pm 0.01$ (Fig. 1).

The pulsed flux above 0.1 GeV, averaged over time, is $F_\gamma = (1.1 \pm 0.1 \pm 0.2) \times 10^{-11}$ erg cm^{-2} s^{-1}, where the first errors are statistical and the second are systematic (SOM). The large distance of NGC 6624 implies that J1823–3021A is one of the most distant γ-ray pulsars detected (*8*). This makes it the most luminous γ-ray MSP to date (*11*): Its total emitted power is $L_\gamma = 4\pi d^2 f_\Omega F_\gamma = (8.4 \pm 1.6 \pm 1.5) \times 10^{34}$ (f_Ω/0.9) erg s^{-1}. We obtained the statistical uncertainty by adding the uncertainties of d and F_γ in quadrature. The term f_Ω is the power per unit surface across the whole sky divided by power per unit surface received at Earth's location; detailed modeling of the γ and radio light curves provides a best fit centered at 0.9, but with a possible range from 0.3 to 1.8 (SOM).

The LAT image of the region around NGC 6624 during the on-pulse interval ($0.60 < \phi < 0.67$ and $0.90 < \phi < 1.07$) shows a bright and isolated γ-ray source that is consistent with the location of J1823–3021A (Fig. 2); in the off-pulse region ($0.07 < \phi < 0.60$ and $0.67 < \phi < 0.90$), no point sources in the energy band 0.1 to 100 GeV are detectable. Assuming a typical pulsar spectrum with a spectral index of 1.5 and a cut-off energy of 3 GeV, we derived, after scaling to the full pulse phase, a 95% confidence level upper limit on the point source energy flux of 5.5×10^{-12} erg cm^{-2} s^{-1}. Thus, J1823–3021A dominates the total γ-ray emission of the cluster. The combined emission of all other MSPs in the cluster, plus any off-pulse emission from J1823–3021A, is not detectable with present sensitivity. No other pulsars are detected in a pulsation search either.

Under the assumption that the γ-ray emission originates from NGC 6624, (*3*) estimated the total number of MSPs to be $N_{MSP} = 103^{+104}_{-46}$.

*All authors with their affiliations appear at the end of the paper.
†To whom correspondence should be addressed. E-mail: pfreire@mpifr-bonn.mpg.de (P.C.C.F.); tyrel.j.johnson@gmail.com (T.J.J.); dmnparent@gmail.com (D.P.); christo.venter@nwu.ac.za (C.V.)